

Inhibition of mammalian target of rapamycin induces phenotypic reversion in three-dimensional cultures of malignant breast epithelial cells

Ross Booth, Soonjo Kwon*, Eric Monson

Department of Biological Engineering, Utah State University, Logan, USA.
Email: soonjo.kwon@usu.edu

Received 27 February 2010; revised 11 March 2010; accepted 17 March 2010.

ABSTRACT

Inhibition of mammalian target of rapamycin (mTOR) is a potential method for cancer treatment. Effects of rapamycin (RAP) on the reversion of malignant breast epithelial cells were investigated on three-dimensional (3D) basement membrane extract (BME) cultures. Through continuous exposure to 20 nM of RAP, cell colony size was significantly reduced in 3D BME cultures of malignant breast epithelial cells, while normal cell colony size appeared unaffected. In unfixed 3D BME cultures of normal and RAP-treated malignant breast epithelial cells, the presence of luminal cell death was confirmed by ethidium bromide and propidium iodide labeling. Increased structural organization was observed by immunofluorescence staining of F-actin and β -catenin in RAP-treated malignant breast epithelial cells. In monolayer cultures of normal and malignant breast epithelial cells, continuous exposure to 20 nM of RAP increased caspase 3/7 activity and decreased proliferation. Reverse transcriptase polymerase chain reaction (RT-PCR) array analysis indicated a fold increase in the expression of a number of proteins related to polarity, cell-cell adhesion, and cell-matrix adhesion in the presence of RAP. Our data showed that phenotypic reversion of malignancy can be achieved through RAP exposure on 3D BME cultures. This 3D BME culture system will provide correct microenvironments for observing the effects of other mTOR inhibitors on phenotypic reversion of malignant breast epithelial cells.

Keywords: Rapamycin; Three-Dimensional Culture; Breast Cancer Reversion; Basement Membrane Extract; mTOR Inhibitors

1. INTRODUCTION

The use of traditional two-dimensional (2D) cultures for

breast cancer studies provides abundant fundamental information on the regulation of breast cancer, but its results often fail to properly translate into clinical applications [1]. The need to effectively address this problem has led to a demand for culture systems which more accurately represent the tissue environment found *in vivo*. In recent years, three-dimensional (3D) culture systems have been developed which use extra-cellular matrix (ECM) proteins [2,3]. 3D cultures provide epithelial cells with spatial freedom to allow the formation of 3D structures. Furthermore, the presence of reconstituted basement membrane extract (BME) promotes polarization of breast epithelial cells into acinar structures with luminal cell death through communication with membrane-bound integrins [3-7]. BME products are derived from the Engelbreth-Holm Swarm (EHS) tumor and are rich in laminin-1, with other ECM components including procollagen IV, heparin sulfate proteoglycan, and entactin [8]. However, most breast cancer cell lines fail to exhibit a normal phenotype in BME cultures unless accompanied with one or more signal molecules [9]. Several signal molecules have previously been shown to affect phenotypic reversion through limited cell proliferation, increased multi-cellular organization, basolateral polarization, and programmed luminal cell death. These reversion factors include inhibitors of β 1-integrin, epidermal growth factor receptor (EGFR), and the MAPK & PI3K kinases [10-12]. Such reversion studies have provided valuable insight for potential methods of cancer treatment.

Rapamycin (RAP), the primary inhibitor for mammalian target of rapamycin (mTOR), has been used for its immunosuppressive properties under the drug name Sirolimus [13]. However, the mTOR signaling pathway has been shown to be a component of several signaling pathways related to breast cancer, including Akt [14], PTEN [15], and PI3K [16]. The web of signaling pathways related to mTOR is complex, and its malignant effects include increased cell growth, proliferation, and

resistance to apoptosis [17]. Presently, RAP and its analogues are under investigation as potential cancer treatments [15]. In breast epithelial cells transformed to exhibit hyperactivity of the Akt kinase, RAP exposure inhibits morphological disruptions caused by Akt overactivity [18]. However, the effects of mTOR inhibition on breast cancer cell lines cultured in 3D BME are not well characterized.

To provide further insight into the value of mTOR inhibition as a potential cancer treatment, we observed and analyzed the phenotypic reversion of malignant breast epithelial cells in 3D BME following exposure to RAP. Two malignant breast epithelial cells (BT-483 and MDA-MB-468) were exposed to RAP and compared to normal breast epithelial cells (184-B5). Changes in multi-cellular morphology, cell proliferation, polarity, and gene expression were investigated in the presence of RAP on 3D BME cultures.

2. MATERIALS AND METHODS

2.1. Cell Culture

Malignant human breast epithelial cells (BT-483 and MDA-MB-468) and normal human breast epithelial cells (184-B5) were purchased from ATCC (VA). For monolayer cultures: BT-483 was cultured using RPMI-1640 (Sigma-Aldrich, MO) with 20% of fetal bovine serum (FBS) (Thermo Fisher Scientific, UT) and 0.01 mg/mL of bovine insulin, MDA-MB-468 was cultured using Leibovitz's L-15 (Sigma-Aldrich) with 10% of FBS in air with no added CO₂, and 184-B5 was cultured using MEGM (Lonza, Switzerland) with 1 ng/mL of cholera toxin. To achieve luminal morphology, cells were cultured using 3D on-top method as previously described [2,3]. 3D culture matrix BME (phenol red free), with reduced growth factors, was obtained from Trevigen (MD). The 3D culture media were modified to contain 2-10% of BME, with 2% of FBS for malignant cells with or without EGF (epidermal growth factor) supplements. All media were supplemented with 1% of Penicillin/Streptomycin (Invitrogen, CA) and 0.1% of Fungizone (Hyclone, UT). Cells were seeded at 0.25×10^5 (184-B5), 0.22×10^5 (BT-483), and 0.18×10^5 (MDA-MB-468) cells/cm². Media were changed every two days subsequent to seeding. RAP (Sigma-Aldrich, MO) was reconstituted in DMSO and stored at -20°C at a stock concentration of 1 µM.

2.2. Morphological Observation

Morphology was observed using a TE2000-S Eclipse Microscope (Nikon, Japan) or a TS100 Eclipse Microscope (Nikon, Japan). All images were taken with a Digital Sight DSQi1Mc Camera (Nikon, Japan). Fluorescence images were detected with an Intensilight C-HGFI lamp (Nikon, Japan). For the detection of

non-viable (apoptotic) cells, non-fixed cultures were incubated for 15-30 minutes with 1 µM of ethidium bromide or 500 nM of propidium iodide and observed for fluorescence. Cell colonies were extracted using PBS-EDTA solution, fixed using 4% of paraformaldehyde, and blocked with 10% of goat serum and 1% of goat F (ab') IgG (Sigma-Aldrich, MO). Monoclonal anti-actin (1A4) and monoclonal anti-β-catenin (15B8) were obtained from Sigma-Aldrich (St. Louis, MO) for use as primary antibodies. Secondary antibody for FITC-conjugated goat anti-mouse was obtained from Santa Cruz Biotechnology (CA). Image analysis was conducted using NIS-Elements v3.0 (Nikon). Areas of cell colonies (in the x-y plane) in all images were analyzed for the calculation of mean areas under different conditions.

2.3. Caspase 3/7 Assay

Monolayers of BT-483 and 184-B5 cells were prepared in a 96-well plate to analyze the effects of RAP on caspase activity. Caspase activity was measured at 24 and 48 hours following exposure to RAP at 0, 5, and 20 nM. One hundred µL of Caspase-Glo 3/7 Reagent (Promega, WI) was added to each sample, including two blank wells containing 100 µL of growth media, and incubated for 2 hours. Luminescence was then measured using a Synergy 4 Plate Reader (Biotek, VT).

2.4. Cell Viability Assay

CellTiter-Blue Cell Viability Assay reagent was obtained from Promega (WI). MDA-MB-468 and 184-B5 cells were seeded in 96-well plates, beginning on day 2, and were treated continuously with 0 nM and 20 nM of RAP. On day three and day seven, cell viability assays were conducted and measured for fluorescence using a Synergy 4 Plate Reader (Biotek, VT).

2.5. Real-Time RT-PCR Arrays

Real time RT-PCR (reverse transcriptase polymerase chain reaction) Arrays for human extracellular matrix and adhesion molecules were obtained from SABiosciences (MD). MDA-MB-468 cells cultured in 3D BME were treated with 0 nM and 20 nM of RAP for 6 days. Cell colonies were extracted using PBS-EDTA, mRNA was extracted using RNeasy RNA isolation kit (QIAGEN, CA), and cDNA synthesis was conducted using the Reverse Transcriptase First Strand Kit (SABiosciences, MD). Real time RT-PCR arrays were run using a Bio-Rad Opticon 2 thermocycler system (MJ Research, Canada) and analyzed using the Opticon 2 software provided. C_t values were acquired graphically.

2.6. Statistical Analysis

With the SYSTAT 12 software, statistical analyses on all quantitative data were carried out using ANOVA (ana-

lyses of variance) to verify statistical significance ($p < 0.05$).

3. RESULTS

3.1. Effects of EGF on Phenotype of Normal Breast Epithelial Cells

Correct signaling from growth factors (EGF) and ECM proteins (BME) contribute to the development and maintenance of a hollow luminal structure within normal human breast epithelial acini, which is schematically described in **Figure 1**. Cells seeded on BME proliferated to form acini. Several events contributing to the formation of a luminal structure preceded the suppression of proliferation within the normal breast epithelial acini. Two populations of cells within each acinus became evident from day 6 to 8: 1) An outer layer of cells that was in direct contact with the matrix and 2) an inner subset of cells that underwent luminal death (apoptosis) (**Figure 1(c)**) and that lacked contact with the matrix. Cells in contact with BME were apparently protected from a global death signal. Normal (184-B5) breast epithelial cells were initially cultured in a MEGM-based medium containing epidermal growth factor (EGF) additive. Resulting cultures contained large, morphologically disrupted structures with no apparent limitations to growth. Culturing the cells in EGF-reduced media resulted in the formation of significantly smaller structures with uniformity in shape (**Figure 2(a)**). The mean area for cell colonies in EGF-reduced media at day 7 was significantly lower than those in EGF-enhanced media at day 7 (**Figure 2(b)**).

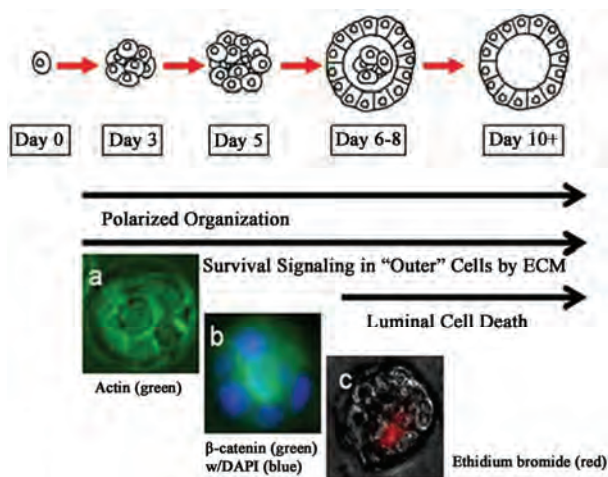
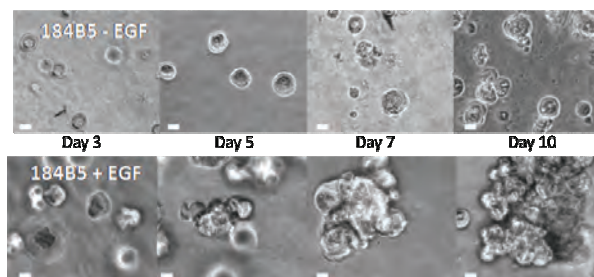
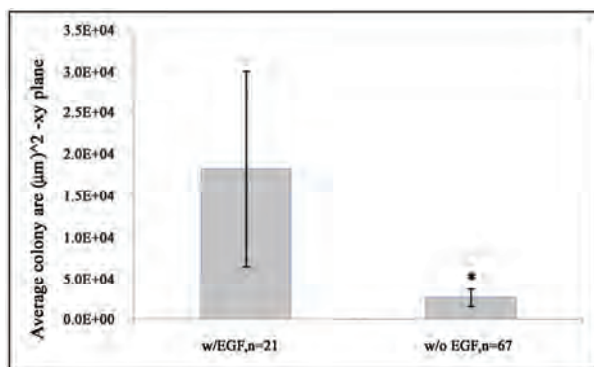


Figure 1. Schematic of biological events during normal human breast epithelial cells' acinar morphogenesis. Normal human breast epithelial cells were cultured using the 3D on-top method. Cell colonies were immunostained against: (a) actin (green); (b) β -catenin (green); (c) ethidium bromide (red). Nuclei were counterstained with DAPI (blue) in (b). Experimental procedures were adapted from [2,3].



(a)



(b)

Figure 2. (a) Effects of EGF-reduction on morphology of normal human breast epithelial cells (184-B5) in 3D BME cultures with and without EGF. Top: EGF-reduced media induced a normal phenotype, including smaller, round morphology with maximum size at day 5 of culture. Bottom: EGF-enhanced media led to increased proliferation and disrupted morphology. (Scale bars = 25 μ m). (b) Effects of EGF on average cell colony size: Average cell colony areas were measured from normal human breast epithelial cells (184-B5) in 3D BME cultures with and without EGF on day 7 of culture. Colonies in EGF-reduced media showed a significantly lower average area than the colonies in EGF-enhanced media. (Error bars \pm st. dev, * significantly lower than control, $p < 0.05$).

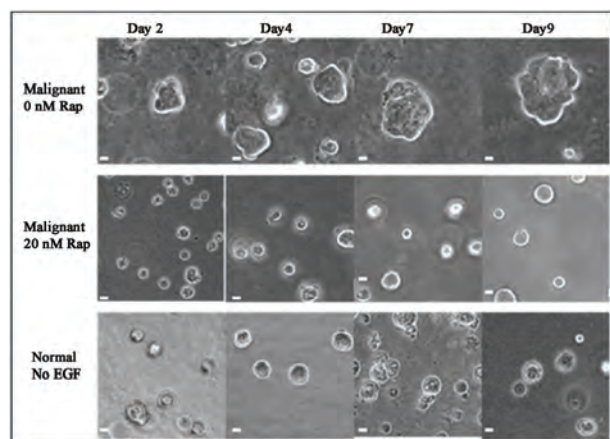
3.2. Effects of RAP Exposure on Malignant Cell Morphology

Morphologies of normal and malignant breast epithelial cells (BT-483 and MDA-MB-468) were compared in 3D BME cultures. Malignant breast epithelial cells did not form organized structures, had no uniformity in shape, and continued to proliferate. Malignant cell colonies exposed to 20 nM of RAP, starting on day 2, formed significantly smaller colonies with a maximum size reached at 6-8 days (**Figure 3(a)**). The mean area for RAP-treated malignant cell colonies was significantly reduced than the untreated malignant cell colonies on day 7 (**Figure 3(b)**).

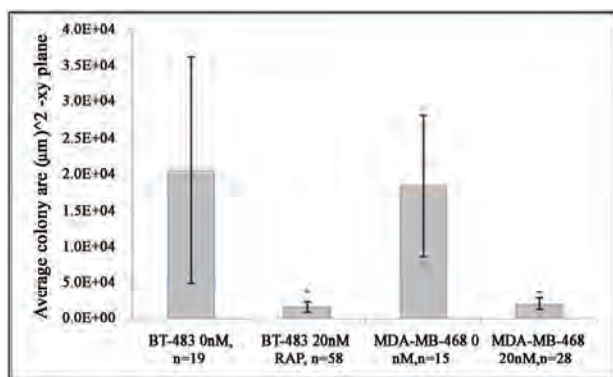
An inner subset of cells undergoing luminal cell death (apoptosis) was observed with ethidium bromide and propidium iodide staining. Apoptotic colonies were commonly found at the center of colonies in normal

(184-B5) breast epithelial cell cultures on day 8, which indicated luminal formation. This was also observed in RAP-treated malignant (BT-483 & MDA-MB-468) cell colonies, providing evidence that the treated malignant breast epithelial cells were reverting to normal phenotypes (**Figure 4(a)**).

Structural organization was also observed using anti-actin and anti- β -catenin immunofluorescence staining (**Figure 4(b)**). RAP-treated malignant colonies exhibited cells arranged around the center, showing similarities to the structure of normal breast epithelial cells in 3D BME

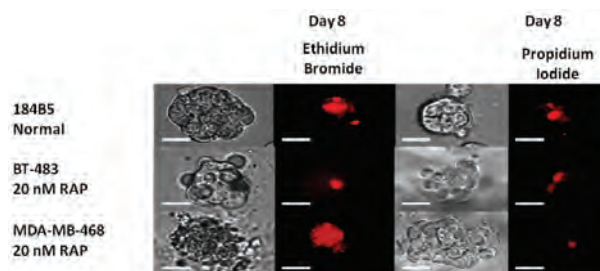


(a)

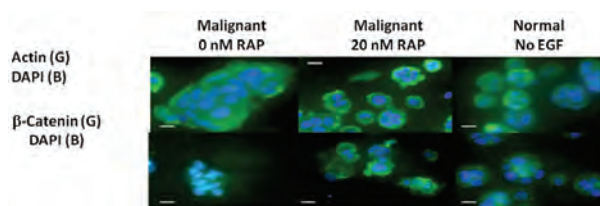


(b)

Figure 3. (a) Comparison of normal, malignant, and RAP-treated malignant human breast epithelial cells in 3D BME culture. RAP was exposed to BT-483 malignant cells beginning on the second day of culture at 0 and 20 nM, and compared to 184-B5 normal cells. Normal cells (bottom) were compared in colony shape and size to RAP-treated malignant cells (middle). Malignant cells (top) exhibited severe morphological disruption when cultured without treatment. (Scale bars = 25 µm); (b) Effects of RAP exposure on average cell colony size: Average cell colony areas were measured from BT-483 and MDA-MB-468 malignant cells treated with 0 and 20 nM of RAP on day 7 of 3D BME culture. No significant difference was found between the two cell lines, but RAP treatment significantly reduced cell colony size of malignant cells. (Error bars \pm st. dev, * significantly lower than control, $p < 0.05$).



(a)



(b)

Figure 4. (a) Selective staining of non-viable cells. Top: Staining of day 8 3D cultures of normal (184-B5) human breast epithelial cells with ethidium bromide or propidium iodide resulted in detection of cell death at the center of cell colonies. Bottom: Similar occurrences of centrally-localized apoptosis were detected in both malignant cell lines when treated continuously with 20 nM of RAP; (b) Immunofluorescence staining of fixed cell colonies from 3D culture. Malignant (BT-483) cell colonies from day 7 of culture, after continuous treatment of 20 nM RAP from day 2, exhibited multi-cellular organization similar to day 7 cultures of normal (184-B5) human breast epithelial cells. Top: Anti-Actin (green) counterstained with DAPI (blue). Bottom: Anti- β -Catenin (green) counterstained with DAPI (blue). (Scale bars = 25 µm)

cultures. Exposure to up to 20 nM of RAP had no apparent effect on the morphology of either EGF-reduced or EGF-enhanced cultures of normal (184-B5) cells (Data not shown).

3.3. Effects of RAP Exposure on Caspase Activity and Proliferation

Confluent monolayers of normal (184-B5) and malignant (BT-483) breast epithelial cells were exposed to RAP at 0, 5, and 20 nM. Caspase activity was measured after 24 and 48 hours of exposure (**Figure 5**). For normal breast epithelial cells, the only condition which showed significant deviation from the control was 20 nM of RAP after 48 hours of exposure (**Figure 5(a)**). For malignant breast epithelial cells, 20 nM of RAP exposure showed a significantly higher effect on caspase activity than 5 nM, but no significant difference was observed with respect to exposure time (**Figure 5(b)**). An increase in caspase activity indicates the presence of programmed cell death, which is essential for the formation of the luminal space in 3D BME cultures.

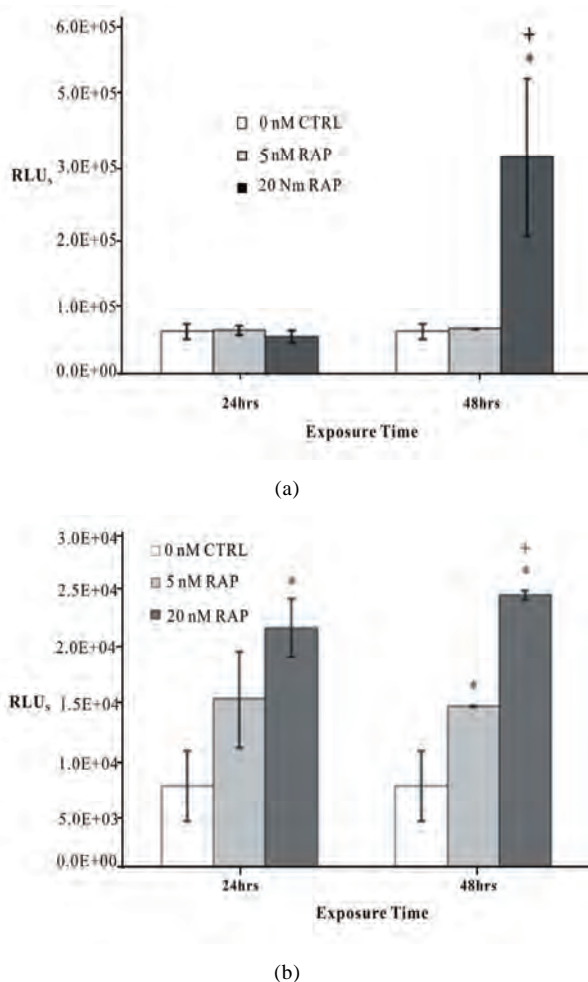


Figure 5. Effect of RAP exposure on caspase activity. (a) Normal human breast epithelial cell monolayers: Caspase activity was measured on samples of 184-B5 exposed to RAP at 5 and 20 nM for 0, 24, and 48 hours following confluency. The only condition which yielded a significant difference from the control group was 20 nM of RAP at 48 hours of exposure. ($n = 2$, * significantly higher than control, + significantly higher than 5 nM, $p < 0.05$); (b) Malignant human breast epithelial cell monolayers: Caspase activity was measured on samples of BT-483 cells exposed to RAP at 5 and 20 nM for 0, 24, and 48 hours following confluency. While there was no significant difference between 24 and 48 hours exposure, all treated samples were significantly higher than the control ($n = 2$, * significantly higher than control, + significantly higher than 5 nM, $p < 0.05$).

RAP's effect on cell proliferation was analyzed in monolayers of normal (184-B5) and malignant (MDA-MB-468) breast epithelial cells (Figure 6) after 2 and 6 days of RAP exposure. Both cell lines showed significantly decreased total cell viability when exposed to 20 nM of RAP, with a significantly higher reduction seen on day 7 (not significant at 5 nM of RAP; data not shown).

3.4. Effects of RAP Exposure on Gene Expression of Extracellular Matrix and Adhesion Molecules

RT-PCR arrays were prepared from malignant breast epithelial cells (MDA-MB-468) in 3D BME cultures containing 0 and 20 nM of RAP on day 6 of culture. Quality controls included with the arrays verified successful RT-PCR and the absence of genomic DNA contamination. C_t values were cut off at > 35 . Genes were grouped into six major classifications, and reported with expression fold change (DDCT method) of untreated controls compared to RAP treated cells (Table 1). In RAP-treated samples, 25 genes related to ECM and adhesion molecules showed a significant (at least 5-fold) increase in expression, while no genes showed a significant decrease in expression (Table 1).

4. DISCUSSION

In this study, the effects of RAP exposure on the phenotypic reversion of malignant breast epithelial cells were investigated in 3D BME culture. Microscopic observation of malignant breast epithelial cells treated with RAP showed greater similarities in morphology to normal cells than in untreated malignant breast epithelial cells in 3D BME cultures. Comparison of the average horizontal area confirmed that RAP-treated malignant cell colonies are significantly smaller in size. Increased structural organization was observed by immunofluorescence staining of anti-Actin and anti- β -Catenin. On day 8 of 3D BME culture, RAP-treated malignant breast epithelial

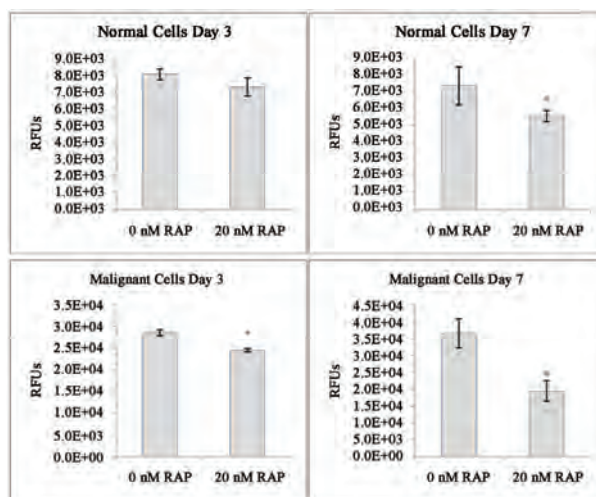


Figure 6. Effect of RAP exposure on total cell viability of normal and malignant human breast epithelial cell monolayers. Cultures of MDA-MB-468 and 184-B5 were exposed to RAP at 0 and 20 nM beginning on the second day of culture. Total cell viability was measured on day 3 and day 7. Both cell lines showed a significant decrease in proliferation at day 7 ($n = 3$, * significantly lower than control, $p < 0.05$).

Table 1. RAP's effects on gene expression of human extracellular matrix and adhesion molecules. Fold change was calculated using the DDCT method, with GADPH as the normalizing gene.

Gene Category	Symbol	Description	Fold Change
Basement Membrane Components	LAMA2	Laminin, alpha 2	13.77
	LAMA3	Laminin, alpha 3	19.05
	LAMB3	Laminin, beta 3	12.57
	SPARC	Secreted protein, acidic, cysteine-rich	13.64
Cell-Cell Adhesion	CDH1	Cadherin 1, type 1, E-cadherin (epithelial)	6.40
	CTNND1	Catenin (cadherin-associated protein), delta 1	7.13
	CD44	CD44 molecule (Indian blood group)	6.95
	ITGA2	Integrin, alpha 2	9.84
	ITGA6	Integrin, alpha 6	5.26
	ITGAV	Integrin, alpha V (vitronectin receptor)	8.99
	ITGB1	Integrin, beta 1 (fibronectin receptor)	14.30
	ITGB2	Integrin, beta 2	9.27
	ITGB5	Integrin, beta 5	5.48
	SGCE	Sarcoglycan, epsilon	5.25
	COL1A1	Collagen, type I, alpha 1	5.79
Other ECM Molecules	COL4A2	Collagen, type IV, alpha 2	9.77
	FN1	Fibronectin 1	16.51
	THBS1	Thrombospondin 1	16.02
	COL12A1	Collagen, type XII, alpha 1	17.50
Other ECM Molecules	CTNNA1	Catenin (cadherin-associated protein), alpha 1	7.82
	CTNNB1	Catenin (cadherin-associated protein), beta 1	11.40
	LAMC1	Laminin, gamma 1 (formerly LAMB2)	6.36
Other ECM Molecules	TGFBI	Transforming growth factor, beta-induced	10.04
	VCAN	Versican	17.70
Trans-membrane Molecules	ITGA4	Integrin, alpha 4	5.87

cells stained with ethidium bromide and propidium iodide showed similar structural organization with luminal cell death to that observed in normal breast epithelial cells, indicating re-polarization of the epithelial cell layers. Supporting data from monolayer cultures indicated that levels of caspase activity were increased in the presence of RAP, and that proliferation over time was decreased. RT-PCR array analysis of RAP-treated malignant breast epithelial cells in 3D BME culture indicated an increase in the expression of several ECM and adhesion molecules important to polarity and structural organization. This collection of data supports our hypothesis that RAP exposure can revert malignant breast epithelial cells to a normal phenotype.

In order to understand why breast cancer develops, as well as to predict the outcome of pharmacological treatments, we need to model the structure and function of organs or tissues in culture so that our experimental manipulations occur under physiological contexts. 3D cultures provide a model to analyze the spatial and temporal aspects of key biological processes (e.g., proliferation and apoptosis) and signal transduction events during morphogenesis. Many of these studies are impractical or impossible to perform in native breast tissue. Cultured normal human breast epithelial cell monolayers in the absence of BME fail to assemble organized structures, and arrest growth when they reach confluence (**Figure 7(a)**). We recently found that signaling from epidermal

growth factor (EGF) and ECM proteins contributes to the development and maintenance of a hollow luminal

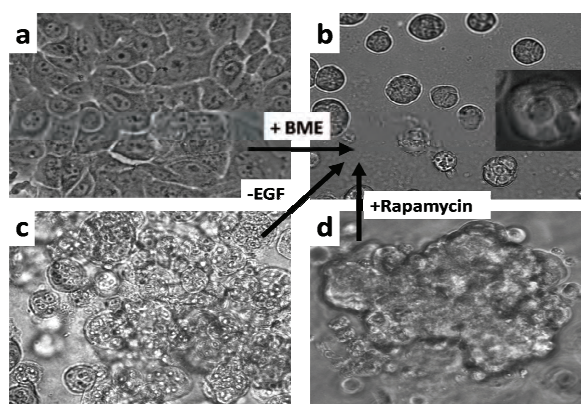


Figure 7. Comparison of normal and malignant human breast epithelial cells grown in 2D monolayer and 3D culture matrix. Normal human breast epithelial cells grown in the 3D BME culture form a luminal structure with normal phenotype (images not to scale). (a) Normal human breast epithelial cells in monolayer without BME (2D); (b) Normal human breast epithelial cells in 3D BME with reduced EGF; (c) Normal human breast epithelial cells in 3D BME with EGF; (d) Malignant human breast epithelial cells in 3D BME with reduced EGF. Phenotypic reversion of malignancy can be achieved through RAP exposure on EGF-reduced 3D BME cultures.

structure within normal breast epithelial acini. In our 3D culture system, non-malignant breast epithelial cells seeded at low density developed into polarized acinar units when EGF is withdrawn. Two populations of cells within each acinus became evident from day 6 to 8: An outer layer of cells that was in direct contact with the ECM, and an inner set of cells not in contact with the matrix that underwent apoptosis (**Figures 1 and 7(b)**). This emulated the ductal structures of breast epithelial cells found in vivo. In the presence of EGF, normal breast epithelial cells exhibited severe morphological deformities, including colony overgrowth, luminal filling, and resistance to apoptosis (**Figure 7(c)**). It was observed that EGF disrupted the formation of luminal structures of normal breast epithelial cells either in monolayer or 3D cultures with BME (**Figures 7(a) and 7(c)**). We also found evidence that rapamycin and its derivative can revert cells' structure from disorganized to organized (**Figures 3, 4, and 7**).

Our criteria for phenotypic reversion are: increased structural organization, limited colony size/proliferation, and the presence of basolateral polarity. Immunofluorescence staining of F-actin and -catenin showed a much higher occurrence of morphologically spherical colonies, indicating structural reorganization. This was also supported by the increase in expression of cell-cell adhesion molecules, transmembrane molecules, and ECM proteases shown by the RT-PCR array data (**Table 1**). Smaller mean area of RAP-treated cell colonies provided strong evidence of limited proliferation. A decreased number of total cell viability over time and increased level of caspase activity confirmed that RAP had a growth-limiting effect on cancer cells. The presence of centrally located cell death indicated the process of lumen formation, directed by caspase-induced programmed apoptosis, and was a result of polarization of the epithelial layers. Up-modulation of caspase, in addition to increased gene expression of basement membrane components and cell-matrix adhesion molecules such as integrins, gave evidence that RAP exposure promoted development of basolateral polarity (**Figure 8**).

In previous studies, RAP has been seen to prevent morphological disruption and inhibit runaway proliferation normally caused by Akt activation in breast epithelial cells (MCF-10A) [18], and to significantly inhibit growth of human lung cancer cells [14]. The value of inhibiting mTOR as a potential cancer treatment was further validated by this study. However, due to its poor water solubility and limited stability, analogues of RAP have been developed with improved pharmaceutical properties for parenteral delivery, including CCI-799 (tensirolimus), RAD-001 (everolimus), and AP-23573 (ARIAD) [15,19,20], which also inhibit mTOR. The effects of these analogues on the phenotypic reversion of malignant breast epithelial cells cultured in 3D BME

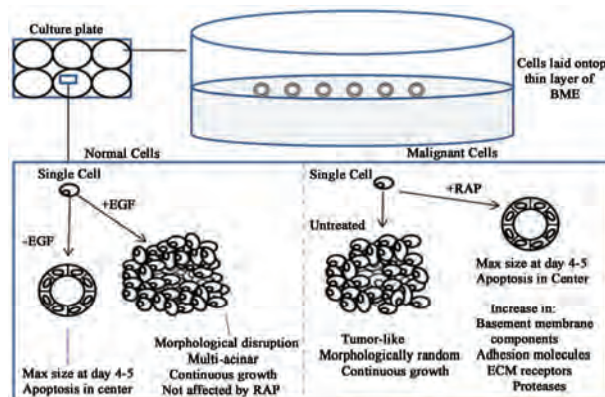


Figure 8. Summary of experimental results. With normal human breast epithelial cells, normal phenotype was achieved by removing EGF additive from the media, leading to limited proliferation, limited cell colony size, and luminal apoptosis. RAP was found to limit proliferation of malignant human breast epithelial cells and induce luminal apoptosis. RT-PCR array data indicated an increase in expression of cell-cell adhesion molecules, transmembrane molecules, and ECM proteases.

should also be studied. Synergistic or additive effects of RAP with other cancer drugs have been studied, including paclitaxel, carboplatin and vinorelbine [21]; mellerian inhibiting substance [22]; doxorubicin [23]; and gemcitabine [24]. Synergistic or additive effects of RAP with other drugs on the phenotypic reversion of malignant cells in 3D BME culture should also be investigated. This study can be used as an experimental template for such future investigation.

In conclusion, by showing that RAP can revert malignant breast epithelial cells to a normal phenotype, our study has provided supporting data for the value of mTOR inhibition as a potential anti-tumor strategy. To provide further insight, two further directions of research should be taken: Further studies on the effects of RAP's analogues on phenotypic reversion, and studies on the synergistic effects of mTOR inhibition with other cancer targets.

5. ACKNOWLEDGEMENTS

Funding for this project was provided by NIH Grant No. 1 R21 CA 131798-01A1. Special thanks to Dr. Timothy Doyle and Dr. David Britt for their contributions.

REFERENCES

- [1] Xu, F. and Burg, K.J. (2007) Three-dimensional polymeric systems for cancer cell studies. *Cytotechnology*, **54(3)**, 135-143.
- [2] Lee, G.Y., Kenny, P.A., Lee, E.H. and Bissell, M.J. (2007) Three-dimensional culture models of normal and malignant breast epithelial cells. *Nature Methods*, **4(4)**, 359-365.
- [3] Debnath, J., Muthuswamy, S.K. and Brugge, J.S. (2003)

- Morphogenesis and oncogenesis of MCF-10A mammary epithelial acini grown in three-dimensional basement membrane cultures. *Methods*, **30**(3), 256-268.
- [4] Roskelley, C.D., Desprez, P.Y. and Bissell, M.J. (1994) Extracellular matrix-dependent tissue-specific gene expression in mammary epithelial cells requires both physical and biochemical signal transduction. *Proceedings of the National Academy of Sciences*, **91**(26), 12378-12382.
- [5] Bello-DeOcampo, D., Kleinman, H.K., Deocampo, N.D. and Webber, M.M. (2001) Laminin-1 and alpha6 beta1 integrin regulate acinar morphogenesis of normal and malignant human prostate epithelial cells. *Prostate*, **46**(2), 142-153.
- [6] Reginato, M.J. and Muthuswamy, S.K. (2006) Illuminating the center: Mechanisms regulating lumen formation and maintenance in mammary morphogenesis. *Journal of Mammary Gland Biology and Neoplasia*, **11**(3-4), 205-211.
- [7] Barcellos-Hoff, M.H., Aggeler, J., Ram, T.G. and Bissell, M.J. (1989) Functional differentiation and alveolar morphogenesis of primary mammary cultures on reconstituted basement membrane. *Development*, **105**(2), 223-235.
- [8] Kleinman, H.K., McGarvey, M.L., Liotta, L.A., Robey, P.G., Tryggvason, K. and Martin, G.R. (1982) Isolation and characterization of type IV procollagen, laminin, and heparan sulfate proteoglycan from the EHS sarcoma. *Biochemistry*, **21**(24), 6188-6193.
- [9] Nelson, C.M. and Bissell, M.J. (2005) Modeling dynamic reciprocity: Engineering three-dimensional culture models of breast architecture, function, and neoplastic transformation. *Seminars in Cancer Biology*, **15**(5), 342-352.
- [10] Liu, H., Radisky, D.C., Wang, F. and Bissell, M.J. (2004) Polarity and proliferation are controlled by distinct signaling pathways downstream of PI3-kinase in breast epithelial tumor cells. *Journal of Cell Biology*, **164**, 603-612.
- [11] Wang, F., Hansen, R.K., Radisky, D., Yoneda, T., Barcellos-Hoff, M.H., Petersen, O.W., Turley, E.A. and Bissell, M.J. (2002) Phenotypic reversion or death of cancer cells by altering signaling pathways in three-dimensional contexts. *Journal of the National Cancer Institute*, **94**(19), 1494-1503.
- [12] Weaver, V.M., Petersen, O.W., Wang, F., Larabell, C.A., Briand, P., Damsky, C. and Bissell, M.J. (1997) Reversion of the malignant phenotype of human breast cells in three-dimensional culture and in vivo by integrin blocking antibodies. *Journal of Cell Biology*, **137**(1), 231-245.
- [13] Sabers, C.J., Martin, M.M., Brunn, G.J., Williams, J.M., Dumont, F.J., Wiederrecht, G. and Abraham, R.T. (1995) Isolation of a protein target of the FKBP12-rapamycin complex in mammalian cells. *Journal of Biological Chemistry*, **270**(2), 815-822.
- [14] Sun, S.Y., Rosenberg, L.M., Wang, X., Zhou, Z., Yue, P., Fu, H. and Khuri, F.R. (2005) Activation of Akt and eIF4E survival pathways by rapamycin-mediated mammalian target of rapamycin inhibition. *Cancer Research*, **65**(16), 7052-7058.
- [15] Vignot, S., Faivre, S., Aguirre, D. and Raymond, E. (2005) mTOR-targeted therapy of cancer with rapamycin derivatives. *Annals of Oncology*, **16**(4), 525-537.
- [16] Heinonen, H., Nieminen, A., Saarela, M., Kallioniemi, A., Klefstrom, J., Hautaniemi, S. and Monni, O. (2008) Deciphering downstream gene targets of PI3K/mTOR/p70S6K pathway in breast cancer. *BMC Genomics*, **9**(4), 348-359.
- [17] Bjornsti, M.A. and Houghton, P.J. (2004) The TOR pathway: A target for cancer therapy. *Nature Reviews Cancer*, **4**(5), 335-348.
- [18] Debnath, J., Walker, S.J. and Brugge, J.S. (2003) Akt activation disrupts mammary acinar architecture and enhances proliferation in an mTOR-dependent manner. *Journal of Cell Biology*, **163**(2), 315-326.
- [19] Gadducci, A., Cosio, S. and Genazzani, A.R. (2006) Old and new perspectives in the pharmacological treatment of advanced or recurrent endometrial cancer: Hormonal therapy, chemotherapy and molecularly targeted therapies. *Reviews in Oncology/Hematology*, **58**(2), 242-256.
- [20] Figlin, R.A., Brown, E., Armstrong, A.J., Akerley, W. and Benson, A.B., Burstein, H.J., Ettinger, D.S., Febbo, P.G., Fury, M.G., Hudes, G.R., Kies, M.S., Kwak, E.L., Morgan, R.J., Mortimer, J.J., Reckamp, K., Venook, A.P., Worden, F. and Yen, Y. (2008) NCCN task force report: mTOR inhibition in solid tumors. *Journal of the National Comprehensive Cancer Network*, **6**(Suppl 5), S1-S20, S21-S22.
- [21] Steelman, L.S., Stadelman, K.M., Chappell, W.H., Horn, S., Basecke, J., Cervello, M., Nicoletti, F., Libra, M., Stivala, F., Martelli, A.M. and McCubrey, J.A. (2008) Akt as a therapeutic target in cancer. *Expert Opinion on Therapeutic Targets*, **12**(9), 1139-1165.
- [22] Pieretti-Vanmarcke, R., Donahoe, P.K., Pearsall, L.A., Dinulescu, D.M., Connolly, D.C., Halpern, E.F., Seiden, M.V. and MacLaughlin, D.T. (2006) Mullerian inhibiting substance enhances subclinical doses of chemotherapeutic agents to inhibit human and mouse ovarian cancer. *Proceedings of the National Academy of Sciences of the USA*, **103**(46), 17426-17431.
- [23] Avellino, R., Romano, S., Parasole, R., Bisogni, R., Lamberti, A., Poggi, V., Venuta, S. and Romano, M.F. (2005) Rapamycin stimulates apoptosis of childhood acute lymphoblastic leukemia cells. *Blood*, **106**(4), 1400-1406.
- [24] Mondesire, W.H., Jian, W., Zhang, H., Ensor, J., Hung, M.C., Mills, G.B. and Meric-Bernstam, F. (2004) Targeting mammalian target of rapamycin synergistically enhances chemotherapy-induced cytotoxicity in breast cancer cells. *Clinical Cancer Research*, **10**(20), 7031-7042.